DOI: 10.18721/JPM.14204
UDC 531.2: 519.63

STABILITY OF AN ELASTIC ORTHOTROPIC CANTILEVER PLATE

M.V. Sukhoterin[1], **T.P. Knysh**[1], **E.M. Pastushok**[1], **R.A. Abdikarimov**[2]

[1] Admiral Makarov State University of Maritime and Inland Shipping,
St. Petersburg, Russian Federation;
[2] Tashkent Financial Institute,
Tashkent, Republic of Uzbekistan

The paper studies the stability of an elastic orthotropic rectangular cantilever plate under compressive forces applied to the face opposite to the seal. The aim of the study was to obtain the range of critical forces and the relevant shapes of the supercritical equilibrium. The deflection function was chosen as a sum of two hyperbolic-trigonometric series with the addition of special compensating terms for the free terms of the Fourier cosine series to the symmetric solution. For the square ribbed plate, the first three critical loads of the symmetric solution and the first critical load of the antisymmetric solution were obtained. The authors present 3D images of the respective equilibrium forms. The results obtained can be used to study the stability of cantilever elements of various structures.

Keywords: orthotropic cantilever plate, stability, Fourier series, critical load, equilibrium form

Citation: Sukhoterin M.V., Knysh T.P., Pastushok E.M., Abdikarimov R.A., Stability of an elastic orthotropic cantilever plate, St. Petersburg Polytechnical State University Journal. Physics and Mathematics. 14 (2) (2021) 37–50. DOI: 10.18721/JPM.14204

УСТОЙЧИВОСТЬ УПРУГОЙ ОРТОТРОПНОЙ КОНСОЛЬНОЙ ПЛАСТИНКИ

М.В. Сухотерин[1], **Т.П. Кныш**[1], **Е.М. Пастушок**[1], **Р.А. Абдикаримов**[2]

[1] Государственный университет морского и речного флота
имени адмирала С.О. Макарова, Санкт-Петербург, Российская Федерация;
[2] Ташкентский финансовый институт,
г. Ташкент, Республика Узбекистан

В работе исследуется устойчивость упругой ортотропной прямоугольной консольной пластинки под действием сжимающих усилий, приложенных к грани, противоположной заделке. Целью исследования является получение спектра критическиих усилий и соответствующих форм закритического равновесия. Функция прогибов выбирается в виде суммы двух гиперболотригонометрических рядов с добавлением к симметричному решению специальных компенсирующих слагаемых для свободных членов разложения функций в ряды Фурье по косинусам. Выполнение всех условий краевой задачи приводит к бесконечной однородной системе линейных алгебраических уравнений относительно неизвестных коэффициентов рядов. Поиск критических нагрузок (собственных чисел), дающих нетривиальное решение этой системы, осуществляется перебором величины сжимающей нагрузки в сочетании с методом последовательных приближений. Для квадратной ребристой пластинки получены первые три критические нагрузки симметричного решения и первая критическая нагрузка антисимметричного решения. Представлены 3D-изображения соответствующих форм равновесия. Результаты работы могут быть использованы для исследования устойчивости консольных элементов различных конструкций.

Ключевые слова: ортотропная консольная пластина, устойчивость, ряд Фурье, критическая нагрузки, форма равновесия

Ссылка при цитировании: Сухотерин М.В., Кныш Т.П., Пастушок Е.М., Абдикаримов Р.А. Устойчивость упругой ортотропной консольной пластинки // Научно-технические ведомости СПбГПУ. Физико-математические науки. 2021. Т. 14. № 2. С. 37–50. DOI: 10.18721/JPM.14204

Introduction

Cantilever plates are used in various fields of technology: in civil and mechanical engineering, shipbuilding and aviation, in instrumentation and control engineering [1] (ferromagnetic plates). Cantilever plates are used in nanotechnology as key sensor components for nanoscale transistors [2], where they are exposed to magnetic fields in the plane of the plate. Cantilever plates are also used in different smart structures [3, 4].

The stability of orthotropic cantilever plates has received insufficient attention this far due to the complexity of the basic differential equation of the problem and the boundary conditions. Reliable numerical analytical methods need to be developed to solve this problem. If we assume the plate material to be perfectly elastic, then there is an infinite number of critical loads that change the form of the plate equilibrium. This eigenvalue problem is similar to the problem on determining the frequency spectrum of free vibrations of a plate [5]. It is primarily interesting from a mathematical standpoint. In practice, only the first critical load (assumed to be load to failure) is computed for planar elements of standard metal structures; however, elastic plates can work in the supercritical region in the presence of structural bending limiters and a rapid increase in the compressive load, acquiring subsequent forms of equilibrium, including antisymmetric ones. Failure may not occur at the first critical load; therefore, it is of practical importance to determine a certain range of critical loads and the corresponding forms of equilibrium.

The stability problem is solved in this study in a linear statement within the theory of thin rigid plates. A more complex nonlinear problem arises for stability of flexible plates; however, linear solutions are used as reference to check the accuracy of the given approximate method.

The stability of anisotropic and isotropic rectangular plates was investigated in [6 – 16] by different means. The methods for solving the buckling problems of anisotropic plates and shells considered in [6 – 9] are also applicable to cantilever plates.

The stability of an isotropic cantilever plate was described in [10, 11] for the cases when a compressive load was applied to a face parallel to the clamped edge [10], and when it was applied to a side face [11]. The first critical loads were found from the condition of the minimum potential energy. Lateral buckling under the action of a concentrated force was also considered in [12] using finite element modeling (FEM). FEM was used in [1] to analyze buckling in ferromagnetic cantilever plates in a magnetic field accounting for plastic deformations.

Anisotropic cantilever nanoplates exposed to in-plane magnetic fields were characterized in [2]. The analytical solution to the linear problem was constructed by a simplex method using trigonometric series. The range of critical forces was obtained for isotropic and orthotropic plates.

FEM and an approximate analytical approach are used in [13] to study the influence that the stiffness of the mid-surface has on the bending of the cantilever plate.

Refs. [14, 15] are dedicated to the stability of an isotropic cantilever plate under the action of compressive forces applied to two parallel free edges [14] or to all three free edges [15]. Two hyperbolic trigonometric series produced an infinite system of linear algebraic equations containing a compressive load as a parameter. Numerical results were obtained for critical loads.

Notably, while FEM has become widespread, it brings the challenge of verifying whether boundary conditions are satisfied. Such verification is fraught with great difficulties, since this numerical method operates arrays of numbers rather than analytical expressions (which can be

substituted into the boundary conditions). FEM is not a universal method for solving mechanical problems and has other drawbacks: insufficient accuracy of solving high-order partial differential equations, computational 'locking' on a refined grid, associated with rounding errors when solving a huge system of linear algebraic equations, 'viewing' of singular points of the solution (stress raisers). The method itself often needs to be verified by purely analytical or numerical analytical methods.

An exact solution to the stability problem has been obtained in our study using hyperbolic trigonometric series with respect to both variables. Satisfying all the conditions of the problem produced an infinite homogeneous system of linear algebraic equations for the coefficients of these series. If the determinant of the system is equal to zero, this yields nontrivial values of the coefficients. However, the procedure for obtaining and solving this equation turns out to be incredibly cumbersome.

We propose a method searching through the load values followed by an iterative process for determining the coefficients. The initial coefficients of the first functional series were given as an arbitrary decreasing sequence; the values of the remaining coefficients were computed next, and they are all refined during the iterative process. The load was selected so that the process converged to nontrivial solutions, that is, adjacent iterations (with nonzero coefficients) did not differ from each other. This load was taken as critical. This method was successfully used in our earlier studies [14, 15].

Problem statement

Let uniform compressive forces with intensity TY be applied to the free edge $Y = b$ of a thin orthotropic rectangular cantilever plate of constant thickness h (Fig. 1). We assume that the main directions of elasticity are parallel to the sides of the plate.

The differential equation of plate stability takes the dimensionless form [16]:

$$D_x \frac{\partial^4 w}{\partial x^4} + 2D_{xy} \frac{\partial^4 w}{\partial x^2 \partial y^2} + \qquad (1)$$

$$+ D_y \frac{\partial^4 w}{\partial y^4} + T_y \frac{\partial^2 w}{\partial y^2} = 0,$$

where w is the relative deflection ($w = W/b$, $W(X,Y)$ is the deflection function of the plate's mid-surface); x, y are the dimensionless coordinates ($x = X/b$, $y = Y/b$); D_x, D_y, D_{xy} are the relative stiffnesses in the principal directions, $D_x = D_1/D$, $D_y = D_2/D$, $D_{xy} = D_3/D$ (D is the cylindrical stiffness of the corresponding isotropic plate of the same thickness, D_1, D_2, D_3 are the principal stiffnesses) T_y is the intensity of relative compressive forces ($T_y = T_Y b^2/D$).

The value D is expressed as

$$D = Eh^3 \Big/ \left[12\left(1-\nu^2\right)\right],$$

where E is Young's modulus of the given plate, ν is its Poisson's ratio.

The main stiffnesses follow the expressions

$$D_1 = E_1 h^3 \Big/ \left[12\left(1-\nu_1\nu_2\right)\right],$$
$$D_2 = E_2 h^3 \Big/ \left[12\left(1-\nu_1\nu_2\right)\right],$$
$$D_3 = D_1\nu_2 + 2D_r,$$

where E_1, E_2, ν_1, ν_2 are the principal elastic constants; Dr is the torsional stiffness, $D_r = Gh^3/12$ (G is the shear modulus).

The relative dimensions of the plate are $\gamma \times 1$, where $\gamma = a/b$.

The boundary conditions are written as follows [16, 17]:
on the face $y = 0$,

$$w = 0, \quad \frac{\partial w}{\partial y} = 0; \qquad (2)$$

on the face $y = 1$,

$$\frac{\partial^2 w}{\partial y^2} + \nu_1 \frac{\partial^2 w}{\partial x^2} = 0,$$

$$D_y \frac{\partial^3 w}{\partial y^3} + \left(D_{xy} + 2\bar{D}_r\right) \frac{\partial^3 w}{\partial x^2 \partial y} + \qquad (3)$$

$$+ T_y \frac{\partial w}{\partial y} = 0;$$

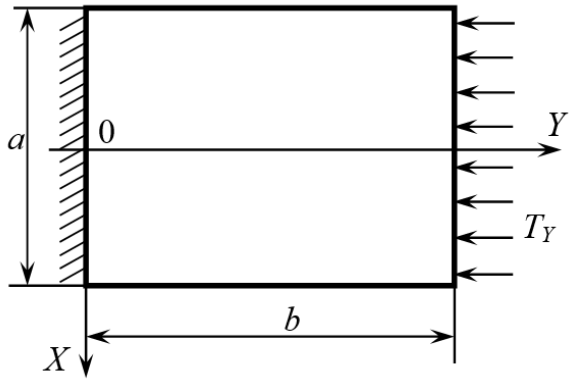

Fig. 1. Loading diagram of cantilever plate (thickness h); T_Y is the intensity of uniform compressive forces

on the faces $x = \pm\gamma/2$,

$$\frac{\partial^2 w}{\partial x^2} + \nu_2 \frac{\partial^2 w}{\partial y^2} = 0,$$
$$D_x \frac{\partial^3 w}{\partial x^3} + \left(D_{xy} + 2\bar{D}_r\right)\frac{\partial^3 w}{\partial x \partial y^2} = 0; \quad (4)$$

at points $(\pm\gamma/2, 1)$,

$$\frac{\partial^2 w}{\partial x \partial y} = 0. \quad (5)$$

Eqs. (2) here are the geometric conditions for rigidly clamped edges (the section does not move or rotate). Eqs. (3), (4) prohibit bending moments and shear forces on the free faces. Condition (5) excludes torques at the corner points of the free part of the boundary. Note that the second condition (3) for shear forces on a face along which a compressive load is applied is complemented with a term accounting for the action of this load in the deflected state of this face. This was pointed out by Alfutov in [17].

Problem (1) – (5) always has a trivial (zero) solution for the deflection function. This corresponds to a stable undeformed state of the plate. Aside from the trivial solution, the problem can also have nontrivial solutions for certain loads Ty, when the plate acquires a new form of equilibrium upon loss of stability. Plates with high elasticity can 'pass' the critical state several times with increasing load, changing the form of the subsequent equilibrium. This refers to plates made of novel highly elastic materials, including nanoplates (graphene).

Construction of the symmetric solution

We represent the sought deflection function as a sum of two series:

$$w_1(x,y) = \sum_{k=1,3,\ldots}^{\infty} \begin{pmatrix} A_k \operatorname{ch}\alpha_k x + \\ + B_k \operatorname{ch}\beta_k x \end{pmatrix} \sin\lambda_k y, \quad (6)$$

$$w_2(x,y) = \\ = \sum_{s=1}^{\infty} (-1)^s \begin{pmatrix} C_s \operatorname{sh}\xi_s \tilde{y} + \\ + H_s \operatorname{sh}\eta_s \tilde{y} + \\ + E_s \operatorname{ch}\xi_s \tilde{y} + \\ + F_s \operatorname{ch}\eta_s \tilde{y} \end{pmatrix} \cos\mu_s x, \quad (7)$$

where A_k, B_k, C_s, H_s, E_s, F_s, α_k, β_k, ξ_s, η_s are undetermined coefficients; $\lambda_k = k\pi/2$; $\mu_s = 2\pi_s/\gamma$; $\tilde{y} = y - 1$.

Notably, both of these functions satisfy the boundary condition (5).

We require that functions (6), (7) satisfy the differential equation (1). This gives biquadratic equations of the following form for the coefficients α_k, β_k, ξ_s, η_s:

$$D_x\alpha_k^4 - 2D_{xy}\alpha_k^2\lambda_k^2 + D_y\lambda_k^4 - T_y\lambda_k^2 = 0,$$
$$D_x\mu_s^4 - 2D_{xy}\xi_s^2\mu_s^2 + D_y\xi_s^4 + T_y\xi_s^2 = 0 \quad (8)$$

(the equations for the coefficients β_k and η_s are similar).

These equations each have four roots, however, based on the properties of hyperbolic functions, it is sufficient to take one pair of roots from each of the quartets:

$$\alpha_k = \lambda_k \sqrt{\frac{D_{xy} + \sqrt{D_{xy}^2 - D_x D_y + \dfrac{D_x T_y}{\lambda_k^2}}}{D_x}}, \quad (9)$$

$$\beta_k = \lambda_k \sqrt{\frac{D_{xy} - \sqrt{D_{xy}^2 - D_x D_y + \frac{D_x T_y}{\lambda_k^2}}}{D_x}},$$

$$\xi_s = \sqrt{\frac{2D_{xy}\mu_s^2 - T_y + R_s}{2D_y}}, \qquad (9)$$

$$\eta_s = \sqrt{\frac{2D_{xy}\mu_s^2 - T_y - R_s}{2D_y}},$$

where

$$R_s = \sqrt{\begin{array}{c} T_y^2 - 4D_{xy}\mu_s^2 T_y + \\ + 4\mu_s^4 \left(D_{xy}^2 - D_x D_y\right) \end{array}}.$$

We now require that the sum of functions (6), (7) satisfy boundary conditions (2) – (4). Then we obtain the following system of equations:

$$\begin{array}{c} C_s \operatorname{sh}\xi_s + H_s \operatorname{sh}\eta_s - \\ - E_s \operatorname{ch}\xi_s - F_s \operatorname{ch}\eta_s = 0, \end{array} \qquad (10)$$

$$\sum_{s=1}^{\infty} (-1)^s \begin{pmatrix} C_s\xi_s \operatorname{ch}\xi_s + \\ + H_s\eta_s \operatorname{ch}\eta_s - \\ - E_s\xi_s \operatorname{sh}\xi_s - \\ - F_s\eta_s \operatorname{sh}\eta_s \end{pmatrix} \cos\mu_s x + \\ + \sum_{k=1,3,\ldots}^{\infty} \lambda_k \left(A_k \operatorname{ch}\alpha_k x + B_k \operatorname{ch}\beta_k x\right) = 0, \qquad (11)$$

$$\sum_{s=1}^{\infty} (-1)^s \begin{bmatrix} E_s\left(\xi_s^2 - \nu_1\mu_s^2\right) + \\ + F_s\left(\eta_s^2 - \nu_1\mu_s^2\right) \end{bmatrix} \cos\mu_s x - \\ - \sum_{k=1,3,\ldots}^{\infty} (-1)^{\tilde{k}} \begin{bmatrix} A_k\left(\nu_1\alpha_k^2 - \lambda_k^2\right)\operatorname{ch}\alpha_k x + \\ + B_k\left(\nu_1\beta_k^2 - \lambda_k^2\right)\operatorname{ch}\beta_k x \end{bmatrix} = 0, \qquad (12)$$

$$\begin{array}{c} C_s\xi_s \left[T_y + D_y\xi_s^2 - \left(D_{xy} + 2\bar{D}_r\right)\mu_s^2\right] + \\ + H_s\eta_s \left[T_y + D_y\eta_s^2 - \left(D_{xy} + 2\bar{D}_r\right)\mu_s^2\right] = 0, \end{array} \qquad (13)$$

$$-\sum_{s=1}^{\infty} \begin{bmatrix} C_s\left(\mu_s^2 - \nu_2\xi_s^2\right)\operatorname{sh}\xi_s\tilde{y} + \\ + H_s\left(\mu_s^2 - \nu_2\eta_s^2\right)\operatorname{sh}\eta_s\tilde{y} + \\ + E_s\left(\mu_s^2 - \nu_2\xi_s^2\right)\operatorname{ch}\xi_s\tilde{y} + \\ + F_s\left(\mu_s^2 - \nu_2\eta_s^2\right)\operatorname{ch}\eta_s\tilde{y} \end{bmatrix} + \\ + \sum_{k=1,3,\ldots}^{\infty} \begin{bmatrix} A_k\left(\alpha_k^2 - \nu_2\lambda_k^2\right)\operatorname{ch}\tilde{\alpha}_k + \\ + B_k\left(\beta_k^2 - \nu_2\lambda_k^2\right)\operatorname{ch}\tilde{\beta}_k \end{bmatrix} \sin\lambda_k y = 0, \qquad (14)$$

$$\begin{array}{c} A_k\alpha_k \left[D_x\alpha_k^2 - \left(D_{xy} + 2\bar{D}_r\right)\lambda_k^2 + \right]\operatorname{sh}\tilde{\alpha}_k + \\ + B_k\beta_k \left[D_x\beta_k^2 - \left(D_{xy} + 2\bar{D}_r\right)\lambda_k^2\right]\operatorname{sh}\tilde{\beta}_k = 0. \end{array} \qquad (15)$$

Here, $\tilde{\alpha}_k = \alpha_k\gamma/2$, $\tilde{\beta}_k = \beta_k\gamma/2$, $\tilde{k} = (k+1)/2$.

Note that the signs of the sum are omitted in Eqs. (10), (13), and (15), since the trigonometric series vanishes when all its coefficients are equal to zero.

Summation in the series in Eqs. (11), (12), (14) is carried out over different indices, so we expand the hyperbolic functions in them into Fourier series. We use the well-known expansions in cos ($\mu_s x$) for Eqs. (11) and (12):

$$\begin{array}{c} \operatorname{ch}\alpha_k x = \\ = \operatorname{sh}\tilde{\alpha}_k \left[\frac{1}{\tilde{\alpha}_k} + \frac{4\alpha_k}{\gamma}\sum_{s=1}^{\infty}(-1)^s \frac{\cos\mu_s x}{\alpha_k^2 + \mu_s^2}\right], \\ \operatorname{ch}\beta_k x = \\ = \operatorname{sh}\tilde{\beta}_k \left[\frac{1}{\tilde{\beta}_k} + \frac{4\beta_k}{\gamma}\sum_{s=1}^{\infty}(-1)^s \frac{\cos\mu_s x}{\beta_k^2 + \mu_s^2}\right]; \end{array} \qquad (16)$$

then these equations (after permutation of the summation signs in the double series) take the form

$$\sum_{s=1}^{\infty} (-1)^s \begin{pmatrix} C_s\xi_s \operatorname{ch}\xi_s + \\ + H_s\eta_s \operatorname{ch}\eta_s - \\ - E_s\xi_s \operatorname{sh}\xi_s - \\ - F_s\eta_s \operatorname{sh}\eta_s \end{pmatrix} \cos\mu_s x + \\ + \varphi_0 + \sum_{s=1}^{\infty} (-1)^s \varphi_s \cos\mu_s x = 0, \qquad (17)$$

$$\sum_{s=1}^{\infty}(-1)^s\begin{bmatrix}E_s\left(\xi_s^2-\nu_1\mu_s^2\right)+\\+F_s\left(\eta_s^2-\nu_1\mu_s^2\right)\end{bmatrix}\cos\mu_s x+ \\ +m_0+\sum_{s=1}^{\infty}(-1)^s m_s\cos\mu_s x=0, \tag{18}$$

where

$$\varphi_0=\sum_{k=1,3,\ldots}^{\infty}\lambda_k\left(A_k\frac{\operatorname{sh}\tilde{\alpha}_k}{\tilde{\alpha}_k}+B_k\frac{\operatorname{sh}\tilde{\beta}_k}{\tilde{\beta}_k}\right),$$

$$\varphi_s=\frac{4}{\gamma}\sum_{k=1,3,\ldots}^{\infty}\lambda_k\left(A_k\frac{\alpha_k\operatorname{sh}\tilde{\alpha}_k}{\alpha_k^2+\mu_s^2}+B_k\frac{\beta_k\operatorname{sh}\tilde{\beta}_k}{\beta_k^2+\mu_s^2}\right),$$

$$m_0=-\sum_{k=1,3,\ldots}^{\infty}(-1)^{\tilde{k}}\begin{bmatrix}A_k\left(\nu_1\alpha_k^2-\lambda_k^2\right)\dfrac{\operatorname{sh}\tilde{\alpha}_k}{\tilde{\alpha}_k}+\\+B_k\left(\nu_1\beta_k^2-\lambda_k^2\right)\dfrac{\operatorname{sh}\tilde{\beta}_k}{\tilde{\beta}_k}\end{bmatrix},$$

$$m_s=-\frac{4}{\gamma}\sum_{k=1,3,\ldots}^{\infty}(-1)^{\tilde{k}}\begin{bmatrix}A_k\left(\nu_1\alpha_k^2-\lambda_k^2\right)\times\\\times\dfrac{\alpha_k\operatorname{sh}\tilde{\alpha}_k}{\alpha_k^2+\mu_s^2}+\\+B_k\left(\nu_1\beta_k^2-\lambda_k^2\right)\times\\\times\dfrac{\beta_k\operatorname{sh}\tilde{\beta}_k}{\beta_k^2+\mu_s^2}\end{bmatrix}. \tag{19}$$

To transform Eq. (14), we use the expansions

$$\operatorname{sh}\xi_s\tilde{y}=-2\sum_{k=1,3,..}^{\infty}\frac{(-1)^{\tilde{k}}\xi_s+\lambda_k\operatorname{sh}\xi_s}{\lambda_k^2+\xi_s^2}\sin\lambda_k y, \\ \operatorname{ch}\xi_s\tilde{y}=2\operatorname{sh}\xi_s\sum_{k=1,3,..}^{\infty}\frac{\lambda_k}{\lambda_k^2+\xi_s^2}\sin\lambda_k y \tag{20}$$

(the expressions for $\operatorname{sh}(\eta_s\tilde{y})$ and $\operatorname{ch}(\eta_s\tilde{y})$ are the same if ξ_s is substituted with η_s) and permute the summation signs in the double series obtained:

$$\sum_{k=1,3,\ldots}^{\infty}b_k\sin\lambda_k y+ \\ +\sum_{k=1,3,\ldots}^{\infty}\begin{bmatrix}A_k\left(\alpha_k^2-\nu_2\lambda_k^2\right)\operatorname{ch}\tilde{\alpha}_k+\\+B_k\left(\beta_k^2-\nu_2\lambda_k^2\right)\operatorname{ch}\tilde{\beta}_k\end{bmatrix}\sin\lambda_k y=0, \tag{21}$$

where

$$b_k=2\sum_{s=1}^{\infty}\begin{bmatrix}\dfrac{\mu_s^2-\nu_2\xi_s^2}{\lambda_k^2+\xi_s^2}\times\\\times\left\{C_s\begin{bmatrix}(-1)^{\tilde{k}}\xi_s+\\+\lambda_k\operatorname{sh}\xi_s\end{bmatrix}-\right\}+\\+\dfrac{\mu_s^2-\nu_2\eta_s^2}{\lambda_k^2+\eta_s^2}\times\\\times\left\{H_s\begin{bmatrix}(-1)^{\tilde{k}}\eta_s+\\+\lambda_k\operatorname{sh}\eta_s\end{bmatrix}-\right\}\end{bmatrix}. \tag{22}$$

Since the free terms φ_0 and m_0 from cosine series expansion appeared in Eqs. (17), (18), we should introduce an auxiliary deflection function w_3, which can compensate for these free terms, satisfying Eqs. (1) – (3), (5) of the problem together with the main solution.

We select this function in the form

$$w_3(y)=\sum_{k=1,3,\ldots}^{\infty}g_k\sin\lambda_k y+\frac{1}{2}My^2-\Phi y, \tag{23}$$

where the coefficients g_k, M, Φ are found from conditions (2) – (4):

$$\sum_{k=1,3,\ldots}^{\infty}g_k\lambda_k^2\left(D_y\lambda_k^2-T_y\right)\sin\lambda_k y+MT_y=0, \\ \sum_{k=1,3,\ldots}^{\infty}g_k\lambda_k-\Phi+\varphi_0=0, \\ \sum_{k=1,3,\ldots}^{\infty}(-1)^{\tilde{k}}\lambda_k^2 g_k+M+m_0=0. \tag{24}$$

We expand the constant $M\cdot T_y$ in the first equation in (25) in a sine Fourier series:

$$MT_y=MT_y\sum_{k=1,3,\ldots}^{\infty}\frac{2}{\lambda_k}\sin\lambda_k y. \tag{25}$$

Then we obtain the following expressions:

$$g_k = \frac{-2MT_y}{\lambda_k^3\left(D_y\lambda_k^2 - T_y\right)},$$

$$M = \frac{-m_0}{1 - 2\sum\limits_{k=1,3,\ldots}^{\infty} \frac{(-1)^{\tilde{k}}\, T_y}{\lambda_k\left(D_y\lambda_k^2 - T_y\right)}}, \qquad (26)$$

$$\Phi = \varphi_0 + \sum_{k=1,3,\ldots}^{\infty} g_k\lambda_k.$$

The residual of the function w_3 with respect to the bending moment M_x on the faces $x = \pm\gamma/2$ (the first condition (4)) is expressed as

$$\nu_2\left(M - \sum_{k=1,3,\ldots}^{\infty} g_k\lambda_k^2 \sin\lambda_k y\right) = \sum_{k=1,3,\ldots}^{\infty} b_k^* \sin\lambda_k y, \qquad (27)$$

where the coefficient

$$b_k^* = \frac{2\nu_2 M D_y\lambda_k}{D_y\lambda_k^2 - T_y} = \frac{-2\nu_2 D_y\lambda_k m_0 \Big/ \left(D_y\lambda_k^2 - T_y\right)}{1 - 2T_y\sum\limits_{k=1,3,\ldots}^{\infty} \frac{(-1)^{\tilde{k}}}{\lambda_k\left(D_y\lambda_k^2 - T_y\right)}} \qquad (28)$$

is added to Eq. (21).

Then system of equations (10) – (15) takes the following final form after the external summation signs are removed, taking into account Eqs. (17), (18), (21), (27):

$$C_s \operatorname{sh}\xi_s + H_s \operatorname{sh}\eta_s - E_s \operatorname{ch}\xi_s - F_s \operatorname{ch}\eta_s = 0, \qquad (29)$$

$$C_s\xi_s \operatorname{ch}\xi_s + H_s\eta_s \operatorname{ch}\eta_s - E_s\xi_s \operatorname{sh}\xi_s - F_s\eta_s \operatorname{sh}\eta_s = -\varphi_s, \qquad (30)$$

$$E_s\left(\xi_s^2 - \nu_1\mu_s^2\right) + F_s\left(\eta_s^2 - \nu_1\mu_s^2\right) = -m_s, \qquad (31)$$

$$C_s\xi_s\left[D_y\xi_s^2 - \left(D_{xy} + 2\bar{D}_r\right)\mu_s^2 + T_y\right] + H_s\eta_s\left[D_y\eta_s^2 - \left(D_{xy} + 2\bar{D}_r\right)\mu_s^2 + T_y\right] = 0, \qquad (32)$$

$$A_k\left(\alpha_k^2 - \nu_2\lambda_k^2\right)\operatorname{ch}\tilde{\alpha}_k + B_k\left(\beta_k^2 - \nu_2\lambda_k^2\right)\operatorname{ch}\tilde{\beta}_k = -\left(b_k + b_k^*\right), \qquad (33)$$

$$A_k\alpha_k\left[D_x\alpha_k^2 - \left(D_{xy} + 2\bar{D}_r\right)\lambda_k^2\right]\operatorname{sh}\tilde{\alpha}_k + B_k\beta_k\left[D_x\beta_k^2 - \left(D_{xy} + 2\bar{D}_r\right)\lambda_k^2\right]\operatorname{sh}\tilde{\beta}_k = 0. \qquad (34)$$

The set (29) – (34) is an infinite homogeneous system of linear algebraic equations with respect to the coefficients A_k, B_k, C_s, H_s, E_s, F_s.

Notice that the right-hand sides φ_s and ms of Eqs. (30), (31) contain the coefficients A_k, B_k under the sum sign (see Eqs. (19)), while the terms on the right-hand side of Eqs. (33) contain, respectively, the coefficients C_s, H_s, E_s, F_s, and also A_k, B_k under the sum signs (see Eqs. (22, 28)). It is extremely complicated to represent a homogeneous system in standard form, to compose and expand the corresponding determinant of the system, to find its roots giving nontrivial solutions; therefore, here we propose a method for enumerating the parameter T_y (the 'shooting' method) combined with the method of sequential approximations for determining the coefficients A_k, B_k, C_s, H_s, E_s, F_s.

To organize the iterative process, the resolving system is divided into two subsystems:

(29) – (32), where the principal coefficients are assumed to be C_s, H_s, E_s, F_s;

(33), (34), where the principal coefficients are assumed to be A_k, B_k.

First, the right-hand side of Eq. (33) is substituted with an initial arbitrary decreasing sequence (in this case, $1/\lambda_k$), then the subsystem of equations (33), (34) is solved for the selected value of the compressive load T_y. The initial coefficients A_{k0}, B_{k0} found are substituted into subsystem (29) – (32), from which the coefficients C_{s0}, H_{s0}, E_{s0}, F_{s0} are found, used then together with A_{k0}, B_{k0} to form the right-hand side of Eq. (33) and a new solution A_{k1}, B_{k1} of systems (33), (34). Next, the first-approximation coefficients C_{s1}, H_{s1}, E_{s1}, F_{s1} are computed, followed by the iterative process of refining the problem coefficients.

If the corresponding coefficients of the series

coincide in absolute value (up to 4–5 significant digits) for the given load starting from some iteration, then this is exactly the nonzero solution of the homogeneous system (29) – (34): its determinant is equal to zero. This (critical) load determines a new form of equilibrium after loss of stability (it corresponds to the minimum potential energy of the plate).

Construction of an antisymmetric solution

We also represent the sought solution as the sum of two series, where odd functions with respect to the variable x appear:

$$w_1(x,y)=\sum_{k=1,3,\ldots}^{\infty}\begin{pmatrix}A_k\,\mathrm{sh}\,\alpha_k x+\\+B_k\,\mathrm{sh}\,\beta_k x\end{pmatrix}\sin\lambda_k y, \qquad (35)$$

$$w_2(x,y)=\\=\sum_{s=1,3,\ldots}^{\infty}(-1)^{\tilde{s}}\begin{pmatrix}C_s\,\mathrm{sh}\,\xi_s\tilde{y}+\\+H_s\,\mathrm{sh}\,\eta_s\tilde{y}+\\+E_s\,\mathrm{ch}\,\xi_s\tilde{y}+\\+F_s\,\mathrm{ch}\,\eta_s\tilde{y}\end{pmatrix}\sin\mu_s x. \qquad (36)$$

Here $\tilde{s}=(s+1)/2$, $\mu_s=\pi s/\gamma$; the coefficients λ_k, α_k, β_k, ξ_s, η_s have the same values as before.

Satisfying all the boundary conditions of the problem, we arrive at a system similar to (29) – (34), but with the sines and cosines interchanged in the last two equations:

$$C_s\,\mathrm{sh}\,\xi_s+H_s\,\mathrm{sh}\,\eta_s-\\-E_s\,\mathrm{ch}\,\xi_s-F_s\,\mathrm{ch}\,\eta_s=0, \qquad (37)$$

$$C_s\xi_s\,\mathrm{ch}\,\xi_s+H_s\eta_s\,\mathrm{ch}\,\eta_s-\\-E_s\xi_s\,\mathrm{sh}\,\xi_s-F_s\eta_s\,\mathrm{sh}\,\eta_s=-\varphi_s, \qquad (38)$$

$$E_s\left(\xi_s^2-\nu_1\mu_s^2\right)+F_s\left(\eta_s^2-\nu_1\mu_s^2\right)=-m_s, \qquad (39)$$

$$C_s\xi_s\left[D_y\xi_s^2-\left(D_{xy}+2\bar{D}_r\right)\mu_s^2\right]+\\+H_s\eta_s\left[D_y\eta_s^2-\left(D_{xy}+2\bar{D}_r\right)\mu_s^2\right]=0, \qquad (40)$$

$$A_k\left(\alpha_k^2-\nu_2\lambda_k^2\right)\mathrm{sh}\,\tilde{\alpha}_k+\\+B_k\left(\beta_k^2-\nu_2\lambda_k^2\right)\mathrm{sh}\,\tilde{\beta}_k=-b_k, \qquad (41)$$

$$A_k\alpha_k\left[D_x\alpha_k^2-\left(D_{xy}+2\bar{D}_r\right)\lambda_k^2\right]\mathrm{ch}\,\tilde{\alpha}_k+\\+B_k\beta_k\left[D_x\beta_k^2-\left(D_{xy}+2\bar{D}_r\right)\lambda_k^2\right]\mathrm{ch}\,\tilde{\beta}_k=0, \qquad (42)$$

where

$$\varphi_s=-\frac{4}{\gamma}\sum_{k=1,3,\ldots}^{\infty}\lambda_k\begin{pmatrix}A_k\dfrac{\alpha_k\,\mathrm{ch}\,\tilde{\alpha}_k}{\alpha_k^2+\mu_s^2}+\\+B_k\dfrac{\beta_k\,\mathrm{ch}\,\tilde{\beta}_k}{\beta_k^2+\mu_s^2}\end{pmatrix},$$

$$m_s=\frac{4}{\gamma}\sum_{k=1,3,\ldots}^{\infty}(-1)^{\tilde{k}}\begin{bmatrix}A_k\left(\nu_1\alpha_k^2-\lambda_k^2\right)\times\\\times\dfrac{\alpha_k\,\mathrm{ch}\,\tilde{\alpha}_k}{\alpha_k^2+\mu_s^2}+\\+B_k\left(\nu_1\beta_k^2-\lambda_k^2\right)\times\\\times\dfrac{\beta_k\,\mathrm{ch}\,\tilde{\beta}_k}{\beta_k^2+\mu_s^2}\end{bmatrix},$$

$$b_k=-2\sum_{s=1,3,\ldots}^{\infty}\begin{bmatrix}\dfrac{\mu_s^2-\nu_2\xi_s^2}{\lambda_k^2+\xi_s^2}\times\\\times\left\{C_s\begin{bmatrix}(-1)^{\tilde{k}}\xi_s+\\+\lambda_k\,\mathrm{sh}\,\xi_s\end{bmatrix}-\right\}+\\+\dfrac{\mu_s^2-\nu_2\eta_s^2}{\lambda_k^2+\eta_s^2}\times\\\times\left\{H_s\begin{bmatrix}(-1)^{\tilde{k}}\eta_s+\\+\lambda_k\,\mathrm{sh}\,\eta_s\end{bmatrix}-\right\}\end{bmatrix}. \qquad (43)$$

Here we used the sine expansion of hyperbolic functions of the variable x in Fourier series:

$$\mathrm{sh}\,\alpha_k x=-\frac{4\alpha_k}{\gamma}\mathrm{ch}\,\tilde{\alpha}_k\sum_{s=1,3,\ldots}^{\infty}(-1)^{\tilde{s}}\frac{\sin\mu_s x}{\alpha_k^2+\mu_s^2},\\\mathrm{sh}\,\beta_k x=-\frac{4\beta_k}{\gamma}\mathrm{ch}\,\tilde{\beta}_k\sum_{s=1,3,\ldots}^{\infty}(-1)^{\tilde{s}}\frac{\sin\mu_s x}{\beta_k^2+\mu_s^2}. \qquad (44)$$

Computations for ribbed plate

As an example, we consider a square plate with closely spaced stiffening ribs placed parallel to the coordinate axes at an equal distance from each other (Fig. 2).

Formulas for calculating the stiffnesses for such a ribbed plate are given in [16]:

$$D_1 = D_2 = D + \frac{E_R I_R}{d}, \quad D_3 = D, \qquad (45)$$

where D is the cylindrical stiffness of the plate itself; E_R, I_R are, respectively, Young's modulus and the moment of inertia of the ribs relative to the midline; d is the distance between the ribs.

Then the relative stiffnesses take the form

$$D_x = D_y = 1 + \bar{D}, \quad D_{xy} = 1 \quad \left(\bar{D} = E_R I_R / dD\right), \qquad (46)$$

and the discriminant of the biquadratic equation (8) (and the similar equation for φ_s and ψ_s) is negative:

$$D_{xy}^2 - D_x D_y = -\left(\bar{D}^2 + 2\bar{D}\right) < 0, \qquad (47)$$

producing complex roots α_k, β_k, φ_s and ψ_s.

The transformations of complex expressions carried out prove that the sought solution is obtained in real form. Computations with the Maple system confirmed this.

We assume that the plate and the ribs are made of the same material. We take Poisson's ratio $\nu = 0.3$, rib width $b_R = h$, rib height $h_R = 3h$, rib width to rib spacing ratio $b_R/d = 0.1$. Then the moment of inertia of the rib and its relative stiffness are expressed as

$$I_R = \frac{b_R h_R^3}{12} - \frac{h^4}{12} = \frac{26}{12} h^4,$$

$$\bar{D} = \frac{E_R I_R}{dD} = \frac{26 E h^4 12\left(1-\nu^2\right)}{12 \cdot 10 h E h^3} = 2{,}6\left(1-\nu^2\right) = 2{,}366.$$

Numerical results

Critical loads and forms of equilibrium were determined according to the above algorithm using Maple software.

The following parameters of the computational process were used:

T_y is the intensity of the relative compressive load applied to the face $y = 1$; $\nu = 0.3$ is Poisson's ratio; $\gamma = a/b$ is the ratio of the sides of the plate; N is the number of terms in the series; N_s is the number of iterations.

The coefficients of series (7), (8) or (36), (37) were printed out at each iteration in order to control the process of successive approximations. After finding the critical value, the deflection function was computed and a $3D$ image of the corresponding form of the plate equilibrium was printed. There were 59 terms retained in a series, a larger number of terms did not significantly affect the accuracy of the computations. The number of iterations was assumed to be 25. The run time for each loading scenario was no more than two minutes. The strategy of enumerating the load was chosen to account for the behavior of the sought coefficient values and did not take much time.

The first three critical loads found for symmetric forms and the first critical loads for the antisymmetric form of equilibrium for square plates (ribbed, with low anisotropy, isotropic) are

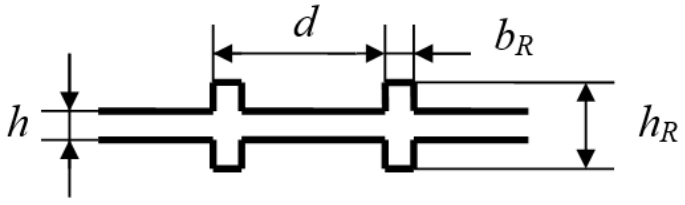

Fig. 2. View of ribbed panel

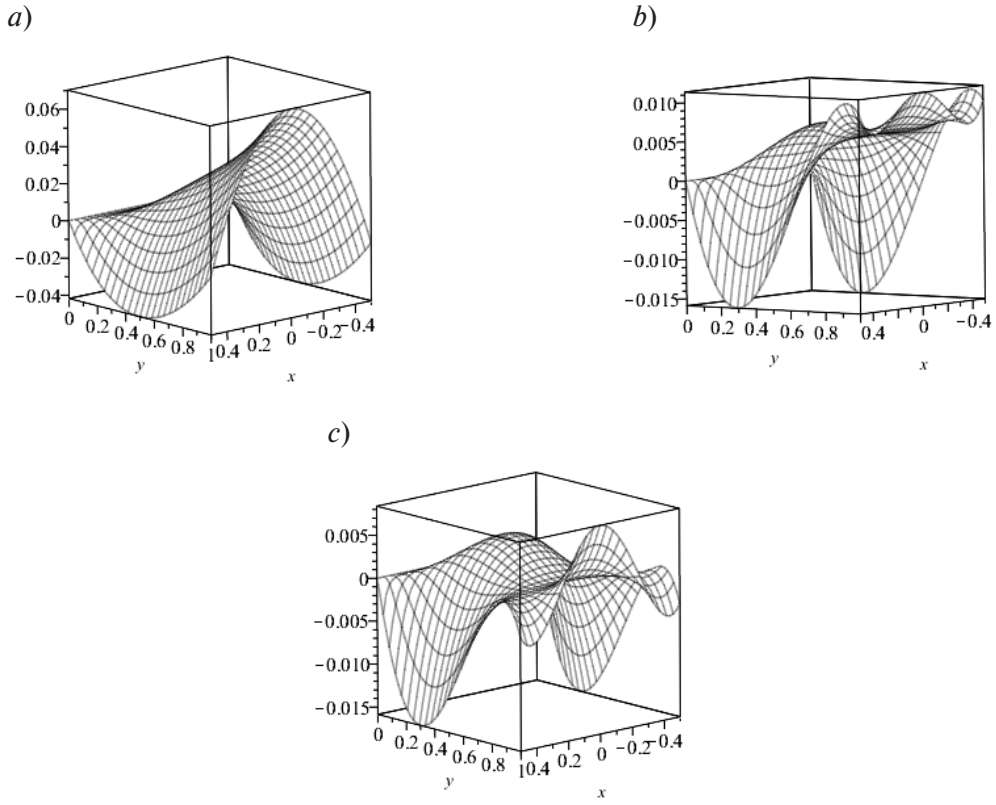

Fig. 3. First (*a*), second (*b*) and third (*c*) symmetrical forms of equilibrium for a ribbed square plate at $T_{cr1} = 7.824$, $T_{cr2} = 64.933$ and $T_{cr3} = 100.970$ respectively

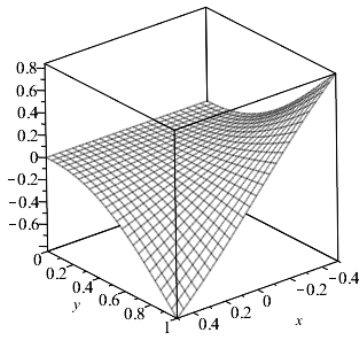

Fig. 4. First antisymmetric form of equilibrium for a ribbed square plate at $T_{cr1} = 25.6765$

shown in Table, and the corresponding 3*D* forms of equilibrium of a ribbed plate are shown in Figs. 3, 4. Importantly, the number of iterations had to be increased to 200 for finding the first antisymmetric critical load due to the weak convergence of the process.

Discussion of computational results

The variation method was used in [10] to find the first critical load for an isotropic square cantilever plate $p_{cr} = 2.4571 \cdot D/a^2$. In this study, the first critical load was computed for comparison for a plate with low anisotropy $\overline{D} = 0.005$, which amounted to $2.1164 \cdot D/a^2$. These values are comparable. We should note that energy methods typically yield overestimated results.

The numerical results in [2] were obtained for the stability of elastic isotropic and orthotropic cantilever nanoplates in a magnetic field using the simplex superposition method based on the

Table

Computed range of critical loads T_y for square cantilever plates

Type of plate	$\bar{D}$	$T_y = T_Y b^2/D$			
		Symmetrical solution			Antisymmetrical solution
		T_{cr1}	T_{cr2}	T_{cr3}	T_{cr1}
Ribbed	2.366	7.8235	64.933	100.970	25.676
With low anisotropy	0.005	2.1164	20.525	58.721	7.835
Isotropic	0	2.1057	20.457	58.597	8.080

Notations: $\bar{D}$ is the relative stiffness of the ribs, T_Y is the intensity of uniform compressive forces, b is the plate length, D is the cylindrical stiffness of the isotropic plate.

nonlocal elasticity theory. Stability computations were performed to verify the method for a very thin (h/a = 1/1000) isotropic cantilever plate but within the framework of the linear Kirchhoff theory. In particular, for a plate with the aspect ratio $\gamma = 2$ subjected to a uniform compressive load applied to the face $y = 1$, the first relative critical values of symmetric forms of equilibrium amounted to (converting these data to the notation we adopted) 2.4174 and 20.5173 versus the values of 2.1594 and 20.663 that we obtained for a standard thin plate (h/a <1/5).

The significant discrepancy (10.7%) for the first critical load can be explained by the large difference in the relative plate thicknesses. Notably, the range of the first six critical loads is given in [2], and the corresponding forms of equilibrium are obtained. This is perhaps the only work on determining the spectrum of eigenvalues and forms in the problem on stability of cantilever plates. On the other hand, however, the buckling in a clamped plate subjected to shear forces along the edge was considered in [18] within the framework of the linear theory; a range of 10 first critical loads and the corresponding 3D forms of equilibrium of plates with different aspect ratios were obtained.

The method proposed in this paper for studying the stability of an elastic orthotropic rectangular cantilever plate allows finding the range of critical loads and the corresponding forms of equilibrium with high accuracy, increasing the number of terms in the series, the number of iterations and the length of the mantissa in the computations.

Conclusion

We have obtained a numerical analytical solution to the stability problem for an elastic rectangular orthotropic cantilever plate. Hyperbolic trigonometric series were used to reduce the problem to an infinite system of linear algebraic equations with respect to unknown coefficients, containing a compressive load as a parameter. An efficient iterative process for finding critical loads has been constructed. A range of critical forces was obtained for a specific example of a ribbed plate; if necessary, it can be expanded by computational means using the Maple environment for numerical analysis. The corresponding 3D forms of equilibrium are given. Finding the critical loads will allow avoiding failure in cantilever elements or understanding their behavior in supercritical regions, offering application for nanotechnology and smart structures.

REFERENCES

1. **Gao Y.,** Analysis on the magneto-elastic-plastic buckling/snapping of cantilever rectangular ferromagnetic plates, Acta Mechanica Solida Sinica. 20 (2007) 180–188.

2. **Wang W., Rong D., Xu C., et al.,** Accurate buckling analysis of magnetically affected canti-

lever nanoplates subjected to in-plane magnetic fields, Journal of Vibration Engineering & Technologies. 8 (4) (2020) 505–515.

3. **Kim J., Varadan V.V., Varadan V.K., Bao X.Q.,** Finite element modeling of a smart cantilever plate and comparison with experiments, Smart Materials and Structures. 5 (2) (1996) 165–170.

4. **Gohari S., Sharifi S., Vrcelj Z.,** A novel explicit solution for twisting control of smart laminated cantilever composite plates/beams using inclined piezoelectric actuators, Composite Structures. 161 (1 February) (2017) 477–504.

5. **Sukhoterin M.V., Baryshnikov S.O., Aksenov D.A.,** Free vibration analysis of rectangular cantilever plates using the hyperbolic-trigonometric series, American Journal of Applied Sciences. 13 (12) (2016) 1442–1451.

6. **Tsiatas G.C., Yiotis A.J.,** A BEM-based meshless solution to buckling and vibration problems of orthotropic plates, Engineering Analysis with Boundary Elements. 37 (3) (2013) 579–584.

7. **Papkov S.O., Banerjee J.R.,** A new method for free vibration and buckling analysis of rectangular orthotropic plates, Journal of Sound and Vibration. 339 (17 March) (2015) 342–358.

8. **Manukhin V.A., Korshunov V.A., Viryacheva N.N.,** O rabotosposobnosti tonkikh plastin posle poteri ustoychivosti [On serviceability of thin plates after buckling], Transactions of the CRI named after acad. A.N. Krylov. (89.2(373)) (2015) 151–160 (in Russian).

9. **Semenov A.A., Moskalenko L.P., Karpov V.V., Sukhoterin M.V.,** Buckling of cylindrical panels strengthened with an orthogonal grid of stiffeners, Bulletin of Civil Engineers. 83 (6) (2020) 117–125 (in Russian).

10. **Xiang-Sheng C.,** The bending stability and vibration of cantilever rectangular plates, Applied Mathematics and Mechanics (English Edition, China). 8 (7) (1987) 673–683.

11. **Xiang-Sheng C.,** On several problems for lateral instability of cantilever plates, Applied Mathematics and Mechanics (English Edition, China). 9 (8) (1988) 787–792.

12. **Jiang L., Wu S., Zheng H.,** Lateral buckling analysis for rectangular cantilever plate subjected to a concentrated load, Advanced Materials Research. 671–674 (2013) 1596–1599.

13. **Yakoob J.A., Hasan I.J.** Study the increasing of the cantilever plate stiffness by using stiffeners, International Journal of Scientific & Engineering Research. 6 (4) (2015) 1678–1687.

14. **Baryshnikov S.O., Sukhoterin M.V., Knysh T.P.,** Stability of external cantilever elements of deep-sea vehicles, Vestnik Gosudarstvennogo Universiteta Morskogo i Rechnogo Flota Imeni Admirala S.O. Makarova. 12 (2 (60)) (2020) 347–358 (in Russian).

15. **Baryshnikov S.O., Sukhoterin M.V., Knysh T.P., Pizhurina N.F.,** Buckling of stabilizers deep-sea vehicles, Marine Intellectual Technologies. 48 (2-1) (2020) 83–90 (in Russian).

16. **Lekhnitskii S.G.,** Anisotropic plates, Gordon and Breach, London, 1968.

17. **Alfutov N.A.,** Stability of elastic structures, Series: Foundations of Engineering Mechanics, Eds.: Babitsky V.I., Wittenburg J., Springer, Berlin, Germany, 2000.

18. **Ullah S., Zhou J., Zhang J., et al.,** New analytic shear buckling solution of clamped rectangular plates by a two-dimensional generalized finite integral transform method, International Journal of Structural Stability and Dynamics. 20 (02) (2020) 2071002.

Received 15.03.2021, accepted 24.05.2021.

THE AUTHORS

SUKHOTERIN Mikhail V.
Admiral Makarov State University of Maritime and Inland Shipping
5/7 Dvinskaya St., St. Petersburg, 198135, Russian Federation
sukhoterinmv@gumrf.ru

KNYSH Tatiana P.
Admiral Makarov State University of Maritime and Inland Shipping
5/7 Dvinskaya St., St. Petersburg, 198135, Russian Federation
knyshtp@gumrf.ru

PASTUSHOK Elena M.
Admiral Makarov State University of Maritime and Inland Shipping
5/7 Dvinskayia St., St. Petersburg, 198135, Russian Federation
pastushokem@gumrf.ru

ABDIKARIMOV Rustamkhan A.
Tashkent Financial Institute
60A, A. Temur St., Tashkent, 100000, Republic of Uzbekistan
rabdikarimov@mail.ru

СПИСОК ЛИТЕРАТУРЫ

1. **Gao Y.** Analysis on the magneto-elastic-plastic buckling/snapping of cantilever rectangular ferromagnetic plates // Acta Mechanica Solida Sinica. 2007. Vol. 20. No. 2. Pp. 180–188.

2. **Wang W., Rong D., Xu C., Zhang Ju., Xu X., Zhou Z.** Accurate buckling analysis of magnetically affected cantilever nanoplates subjected to in-plane magnetic fields // Journal of Vibration Engineering & Technologies. 2020. Vol. 8. No. 4. Pp. 505–515.

3. **Kim J., Varadan V.V., Varadan V.K., Bao X.Q.** Finite element modeling of a smart cantilever plate and comparison with experiments // Smart Materials and Structures. 1996. Vol. 5. No. 2. Pp. 165–170.

4. **Gohari S., Sharifi S., Vrcelj Z.** A novel explicit solution for twisting control of smart laminated cantilever composite plates/beams using inclined piezoelectric actuators // Composite Structures. 2017. Vol. 161. 1 February. Pp. 477–504.

5. **Sukhoterin M.V., Baryshnikov S.O., Aksenov D.A.** Free vibration analysis of rectangular cantilever plates using the hyperbolic-trigonometric series // American Journal of Applied Sciences. 2016. Vol. 13. No. 12. Pp. 1442–1451.

6. **Tsiatas G.C., Yiotis A.J.** A BEM-based meshless solution to buckling and vibration problems of orthotropic plates // Engineering Analysis with Boundary Elements. 2013. Vol. 37. No. 3. Pp. 579–584.

7. **Papkov S.O., Banerjee J.R.** A new method for free vibration and buckling analysis of rectangular orthotropic plates // Journal of Sound and Vibration. 2015. Vol. 339. 17 March. Pp. 342–358.

8. **Манухин В.А., Коршунов В.А., Вирячева Н.Н.** О работоспособности тонких пластин после потери устойчивости // Труды ЦНИИ им. акад. А.Н. Крылова. 2015. Т. 89. № 2. С. 151–160.

9. **Семенов А.А., Москаленко Л.П., Карпов В.В., Сухотерин М.В.** Устойчивость цилиндрических панелей, подкрепленных ортогональной сеткой ребер // Вестник гражданских инженеров. 2020. Т. 83. № 6. С. 117–125.

10. **Xiang-Sheng C.** The bending stability and vibration of cantilever rectangular plates // Applied Mathematics and Mechanics (English Edition, China). 1987. Vol. 8. No. 7. Pp. 673–683.

11. **Xiang-Sheng C.** On several problems for lateral instability of cantilever plates // Applied Mathematics and Mechanics (English Edition, China). 1988. Vol. 9. No. 8. Pp. 787–792.

12. **Jiang L., Wu S., Zheng H.** Lateral buckling analysis for rectangular cantilever plate subjected to a concentrated loads // Advanced Materials Research. 2013. Vols. 671–674. Pp. 1596–1599.

13. **Yakoob J.A., Hasan I.J.** Study the increasing of the cantilever plate stiffness by using stiffeners // International Journal of Scientific & Engineering Research. 2015. Vol. 6. No. 4. Pp. 1678–1687.

14. **Барышников С.О., Сухотерин М.В., Кныш Т.П.** Устойчивость внешних консольных элементов глубоководных аппаратов // Вестник государственного университета морского и речного флота им. адмирала С.О. Ма-

карова. 2020. Т. 12. № 2. С. 347–358.

15. **Барышников С.О., Сухотерин М.В., Кныш Т.П., Пижурина Н.Ф.** Устойчивость стабилизаторов глубоководных аппаратов // Морские интеллектуальные технологии. 2020. Т. 48. № 2-1. С. 83–90.

16. **Лехницкий С.Г.** Анизотропные пластинки. Москва-Ленинград: Гостехиздат, 1947. 355 с.

17. **Алфутов Н.А.** Основы расчета на устойчивость упругих систем. М.: Машиностроение, 1991. 334 с.

18. **Ullah S., Zhou J., Zhang J., Zhou C., Wang H., Zhong Y., Wang B., Li R.** New analytic shear buckling solution of clamped rectangular plates by a two-dimensional generalized finite integral transform method // International Journal of Structural Stability and Dynamics. 2020. Vol. 20. No. 02. P. 2071002.

Статья поступила в редакцию 15.03.2021, принята к публикации 24.05.2021.

СВЕДЕНИЯ ОБ АВТОРАХ

СУХОТЕРИН Михаил Васильевич – *доктор технических наук, член-корреспондент РАЕ, заведующий кафедрой Государственного университета морского и речного флота имени адмирала С.О. Макарова, Санкт-Петербург, Российская Федерация.*

198135, Российская Федерация, г. Санкт-Петербург, Двинская ул., 5/7

sukhoterinmv@gumrf.ru

КНЫШ Татьяна Петровна – *кандидат физико-математических наук, заместитель начальника управления информатизации Государственного университета морского и речного флота имени адмирала С.О. Макарова, Санкт-Петербург, Российская Федерация.*

198135, Российская Федерация, г. Санкт-Петербург, Двинская ул., 5/7

knyshtp@gumrf.ru

ПАСТУШОК Елена Михайловна – *доцент Государственного университета морского и речного флота имени адмирала С.О. Макарова, Санкт-Петербург, Российская Федерация.*

198135, Российская Федерация, г. Санкт-Петербург, Двинская ул., 5/7

pastushokem@gumrf.ru

АБДИКАРИМОВ Рустамхан Алимханович – *доктор физико-математических наук, профессор Ташкентского финансового института, г. Ташкент, Республика Узбекистан.*

100000, Республика Узбекистан, г. Ташкент, ул. А. Темур, 60А

rabdikarimov@mail.ru